# Time-Code-Spatial Modulated IRS-Aided Radar Localization in NLoS Scenario

Yuan Liu, Moein Ahmadi, Johann Fuchs, and M. R. Bhavani Shankar
Interdisciplinary Centre for Security, Reliability and Trust (SnT), University of Luxembourg, L-1855, Luxembourg
Email: {yuan.liu, moein.ahmadi, johann.fuchs, bhavani.shankar }@uni.lu

***Abstract*—Following the developments in wireless communications, the use of intelligent reflecting surfaces (IRS) to extend radar illumination to non-line-of-sight (NLoS) scenarios has spurred research interest of late. Initial works have assumed ideal propagation conditions based on the radar equation to assess the signal noise ratio (SNR) enhancement. In this paper, we consider a realistic target position estimation of an IRS-aided radar system framework. Firstly, a time-code-space (TCS) IRS array model was proposed, where each sub-unit array can work independently as a TX IRS unit or Rx IRS unit. Then, the signal model of the time division multiplexing (TDM) IRS array based on the frequency-modulated continuous waveform (FMCW) is derived. Thereafter, the developed signal model is used to emulate the radar performance utilizing a Blender-based simulator in NLoS scenarios, where the various assumptions commonplace in literature and their suitability in realistic scenarios are considered. The simulation result shows the validation of the proposed IRS-aided framework in target localization. Further, the trade-off between angle resolution and energy/ time consumption is also discussed.**

***Index Terms*—Blender, IRS-aided radar, NLoS localization, time-code-spatial modulated IRS, TDM IRS array.**

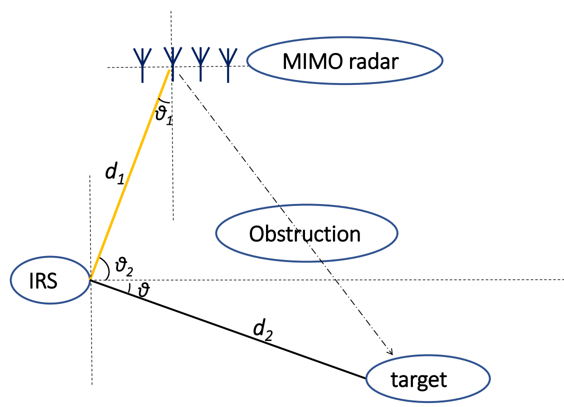


Fig. 1. IRS assisted radar in NLoS scenarios.

## I. Introduction

Intelligent Reflecting Surfaces (IRS) have been used in communication systems for signal-to-noise (SNR) ratio enhancement [1], capacity increase [2], and radio-based localization [3] by controlling the radio waves in frequency, amplitude, phase, polarization, and propagation direction [4], [5], [6]. Recently, IRS is being considered for assisting the radar systems in non-line-of-sight (NLoS) scenarios [7], and the merits of signal enhancement in IRS-aided multiple inputs multiple outputs (MIMO) radar systems have already been analyzed [8]. However, very few papers discuss localization and tracking in an IRS-aided radar system.

Conventionally the MIMO radar is used in range-angle estimation by utilizing the phase difference due to the spatial geometry of the array [9], [10]. However, this requires the LoS path between the radar and the target. When the LoS path between the radar and the target is obstructed, the IRS can aid in establishing the virtual LoS links in a NLoS scenario as shown in Fig.1 for an IRS-aided co-located MIMO radar system. However, creation of the virtual LoS paths does not implicitly enable angle estimation. Referring to Fig.1, under the far-field assumption, the phase difference between the incident waves at the radar receiver elements enables estimation of the angle of arrival (AoA) $\theta_1$. However, the $\theta_1$ is already known since the deployment of the radar and the IRS are known. The parameter of interest is the estimation of $\theta$, where the IRS needs to be operationalized to work as an array. In this context, in addition to the conventional IRS, recent works on metasurfaces promote the function of the passive IRS to incorporate time multiplexing of smaller sub-units through time coding [11]. For example, [12] eliminates the sideband and the harmonic frequencies due to the time slot switching, and achieves 1-bit time modulated time-code-space (TCS) metasurfaces, i.e., to switch-on or switch-off the sub-unit of the IRS within the desired time slots. Therefore, it is possible to control the IRS to work as an array, where each sub-unit works orthogonally in time.

In this paper, we propose a novel time division multiplexing (TDM) IRS-aided frequency modulated continuous waveform (FMCW) radar framework for target position estimation. The detailed contributions resulting in the aforementioned framework include: (i) identification of the concept that for angle estimation in NLoS scenarios, an array operation at the IRS is necessary rather than a MIMO radar; (ii) formulation of the mathematical model of the IRS array and derive the AoAs and the angle of departures (AoDs) at IRS array; (iii) derive the time division multiplexing (TDM) IRS array signal model based on FMCW and relate it to the classical LoS literature, (iv) utilize an environment-based signal simulator, *Blender*, for validation.

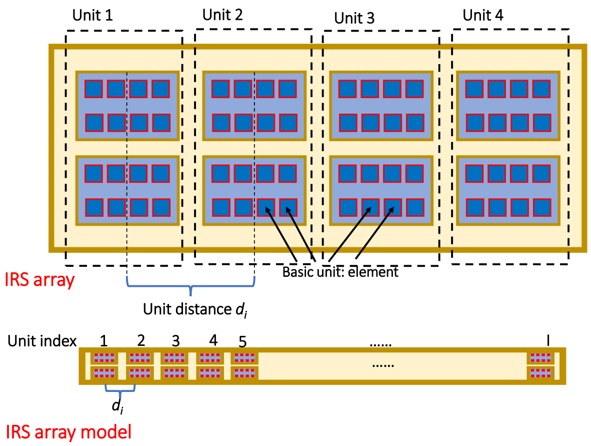


Fig. 2. The illustration of the IRS array and model.

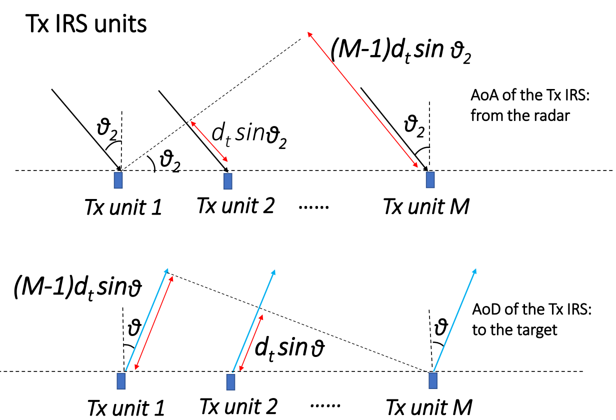


Fig. 3. Illustration of delay difference due to the spatial geometry at the Tx IRS units.

## II. Signal Model

### A. The IRS array

The structure of the IRS array is illustrated in Fig.2, where an IRS array is divided into multiple IRS units with each unit consisting of hundreds of elements. Each IRS unit is capable of independent spatial beam-forming and the resulting IRS can be considered as a linear array (LA) consisting of several IRS units. Fig.2 illustrates four IRS units as an example, where the distance $d_i$ between neighboring IRS units is controllable. Considering the scenario in Fig.1, with the MIMO radar replaced by a single antenna radar, and a single IRS replaced by an IRS array with $M+N$ units. The $M$ units spaced at a distance $d_t$ are used only for transmitting the radar signal to the target and are henceforth referred to as Tx IRS units. The $N$ units spaced at a distance $d_r$ are used only for receiving the scattered signal from the target and beamforming it to the radar, these are referred to as Rx IRS units.

Based on the angle information of Fig.1, the AoAs $\theta_2$ and the AoD $\theta$ of the Tx IRS units are illustrated in Fig.3, hence

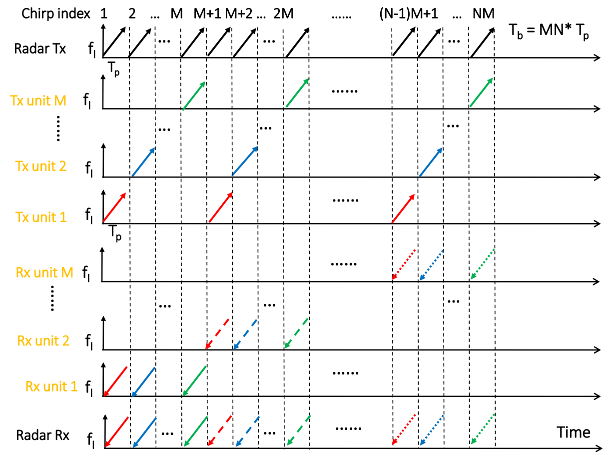


Fig. 4. Illustration of FMCW used in TDM IRS-array aided radar in one CPI block.

the delay difference due to the array geometry at the $m$th Tx IRS unit is the addition of AoA and AoD as

$$\Delta d_{tx,m} = -(m-1)d_t \sin\theta_2 + (M-m)d_t \sin\theta. \quad (1)$$

Similarly, the delay difference at the $n$th Rx IRS unit is

$$\Delta d_{rx,n} = -(n-1)d_r \sin\theta_2 + (N-n)d_r \sin\theta. \quad (2)$$

Due to the $\sin(\cdot)$ term, the delay is not a linear function of the corresponding angle. To eliminate the term with $\sin\theta_2$, we apply phase shift $\exp\{j\psi_m(t)\}$ and $\exp\{j\psi_n(t)\}$ on the $m$th Tx IRS units and the $n$th Tx IRS units, respectively.

$$\psi_m(t) = 2\pi f(t)\frac{(m-1)d_t \sin\theta_2}{c}, \quad (3)$$

$$\psi_n(t) = 2\pi f(t)\frac{(n-1)d_r \sin\theta_2}{c}, \quad (4)$$

where $f(t)$ denotes the time-varying carrier frequency of FMCW and $c$ is the speed of light.

By spacing the $d_t = Nd_r$, we could obtain an $M$ by $N$ virtual array after the elimination of the $\theta_2$ terms.

### B. Signal model of the TDM-IRS aided SISO radar

Considering the IRS-aided single input single output (SISO) radar in Fig.1, where the LoS between radar antennas and the target is obstructed. To estimate the angle of the target, the IRS is replaced by the IRS array, with $M$ Tx IRS units and $N$ Rx IRS units. To separate signals from the IRS array at the radar side, the classic TDM technique is applied to this IRS array, where the timing diagram of the whole IRS-array-aided radar system is shown in Fig.4. The radar antenna radiates the FMCW signal consecutively with the chirp time $T_p$, each Tx IRS unit sequentially transmits one chirp to the target in orthogonal time, and each Rx IRS unit sequentially receives $M$ chirps from the target and sends them to the radar in orthogonal time. A coherent processing interval (CPI) consists of $L$ TDM blocks, and a block consisting of $MN$ chirp times, i.e., $T_b = MNT_p$ represented in Fig.4.

Based on the designed waveform slots, the transmitted FMCW signal by the radar is

$$\boldsymbol{s}(t;l) = \sum_{m=1}^{M}\sum_{n=1}^{N}\sqrt{\frac{P_0}{2}} \exp\{j\phi(t-[(n-1)M+m-1]T_p-(l-1)T_b)\}, \tag{5}$$

$$\text{with} \quad \phi(t) = 2\pi(f_l t + \frac{1}{2}\mu t^2) - \phi_0, \tag{6}$$

where $m$ and $n$ are the indices of the Tx IRS unit and Rx IRS unit respectively, representing the radar signal is transmitted to the target via the $m$th Tx IRS unit, and the scattering signal from the target is sent back to the radar via the $n$th Rx IRS unit, $l = 1, 2, ..., L$ is the index of CPI block, $P_0$ is the transmitted power, $f_l$ is the starting frequency, $\mu = B/T_p$ is the FMCW slope with $B$ representing the bandwidth, $T_p$ representing one chirp duration, $T_b$ denoting the one CPI block time, $t \in [(l-1)T_b, lT_b]$.

The signal at the radar receive antenna is represented as

$$\begin{aligned}\boldsymbol{r}(t;l) = &\sum_{m=1}^{M}\sum_{n=1}^{N}\sqrt{\frac{P_{m,n}}{2}}\exp\{j\psi_m(t)\}\exp\{j\psi_n(t)\}\\ &\exp\{j\phi(t-[(n-1)M+m-1]T_p\\ &-(l-1)T_b-\tau_{m,n}\},\end{aligned} \tag{7}$$

where $\sqrt{\frac{P_{m,n}}{2}}$ is the received amplitude, containing the radar cross section (RCS), the IRS gain, and the attenuation of propagation channel corresponding to the radar, the $m$th IRS Tx unit, the $n$th IRS Rx unit, and the target. The propagation delay $\tau_{m,n}$ can be calculated as

$$\tau_{m,n} = \frac{d_{m,n} + 2v_l t}{c}, \tag{8}$$

$v_l$ is the absolute speed between the target and the IRS array, $d_{m,n}$ denotes the distance, decided by the reference distance and the delay due to the IRS array geometry defined in (1) and (2) as

$$d_{m,n} = 2(d_1 + d_2) + \Delta d_{tx,m} + \Delta d_{rx,n}. \tag{9}$$

Considering the IRS phase shift $\psi_m(t)$ and $\psi_n(t)$ which are defined in (3) and (4), the two terms $\tau_{m,n} + \psi_{m,n}$ can be simplified, hence the received signal in (7) can be rewritten as

$$\boldsymbol{r}(t;l) = \sum_{m=1}^{M}\sum_{n=1}^{N}\sqrt{\frac{P_{m,n}}{2}}\exp\{ j\phi(t-[(n-1)M+m-1]T_p-(l-1)T_b-\tau'_{m,n}\}, \tag{10}$$

$$\tau'_{m,n} = 2\frac{R_{m,n}+v_l t}{c}, \tag{11}$$

$$R_{m,n} = (d_1+d_2)+(M-m)d_t\sin\theta+(N-n)d_r\sin\theta. \tag{12}$$

Here, $d_2$ and $\theta$ are the unknown parameters of the target to be estimated. By controlling the distance of IRS unit $d_t = \lambda/2$, and $d_r = Md_t$, we have the virtual array for angle estimation.

The mixer is used to down-convert the radio frequency (RF) signals to the intermediate frequency (IF) signals at the radar side, thereafter the beat signal is obtained by sampling the IF signals [13], [14]. The beat signal of the radar receiver can be represented as $\boldsymbol{h} \in \mathbb{C}^{L\times N_s}$, where $L$ denotes the number of chirps in one CPI and $N_s$ denotes the number of samples in one chirp, and the and the $(l, n_s)$-th entry can be expressed as

$$\boldsymbol{h}(l,n_s) = \sum_{m=1}^{M}\sum_{n=1}^{N} A_{if,m,n}\exp\{j2\pi( \frac{2\mu R_{m,n}}{c}\frac{n_s-1}{F_s} - f_D(l-1)T_b+\phi_1)\}, \tag{13}$$

where $A_{if,m,n}$ denotes the IF signal strength corresponding to the $l$th chirps between the $m$th Tx and the$n$th Rx, $c$ is the speed of the light, $n_s$ is the index of sampling number, $F_s$ is the sampling frequency, $\phi_1$ is a constant, $f_D$ represents the Doppler shift due to the velocity $v$ of the target as

$$f_D = -2\frac{f_l v}{c} \text{ and,} \tag{14}$$

$$R_{m,n} = R_0 + \frac{\lambda}{2}((N-n)M+(M-m))\sin\theta, \tag{15}$$

where $R_0$ is the reference distance between the target and the MIMO, and $\theta$ is the AoA.

For TDM-IRS-aided radar, the channels via different Tx and Rx IRS units can be separated by the chirp index. In particular, each block contains $MN$ time orthogonal chirps and the channel corresponding to the $m$th Tx, $n$th Rx IRS unit $\boldsymbol{h}_{m,n} \in \mathbb{C}^{[L/(MN)]\times N_s}$ can be separated by the chirp index as

$$\boldsymbol{h}_{m,n}[\hat{l},:] = \boldsymbol{h}[(m+(n-1)M+(\hat{l}-1)MN),:], \tag{16}$$

where $L/(MN)$ is the number of chirps in one CPI, and the chirp index $\hat{l}$ is expressed as

$$\hat{l} = 1, 2, ..., \frac{L}{MN}. \tag{17}$$

where $\boldsymbol{h}[l,:]$ denotes the $l$th row of matrix $\boldsymbol{h}$.

## III. Validation via Environment-based simulation

The environment-based radar signals are used for the validation of the proposed IRS-aided target estimation framework, where the image animation tool called Blender is used for environment modeling and tracing the propagation paths of the channel, and then radar signals are generated based on the channel models. Readers interested in the principle of the Blender-based radar simulation could refer to [15], [16].

The IRS-assisted radar scenario is shown in Fig.5, where the LoS paths between the radar and the targets are obstructed by a wall; hence the radar signal could be assisted by the IRS array. However, there is no IRS model in the state of the art in Blender, hence we separate the synthetic channel of the entire radar-IRS-target link into three sub-channels as shown in the Fig.6, the $\boldsymbol{h}_{m,n}$ in (16) can be separated into three parts. The $(\hat{l}, n_s)$-th entry of $\boldsymbol{h}_{m,n}$ can be calculated as

$$\boldsymbol{h}_{m,n}(\hat{l},n_s) = \boldsymbol{h}_{R,n}(\hat{l},n_s)\boldsymbol{h}_{irs,m,n}(\hat{l},n_s)\boldsymbol{h}_{T,m}(\hat{l},n_s), \tag{18}$$

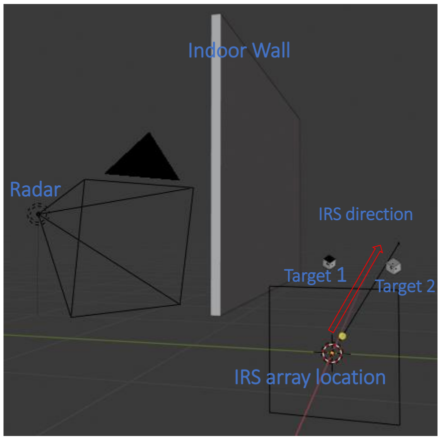


Fig. 5. Illustration of the simulation scenario with radar, IRS array, and the targets in Blender.

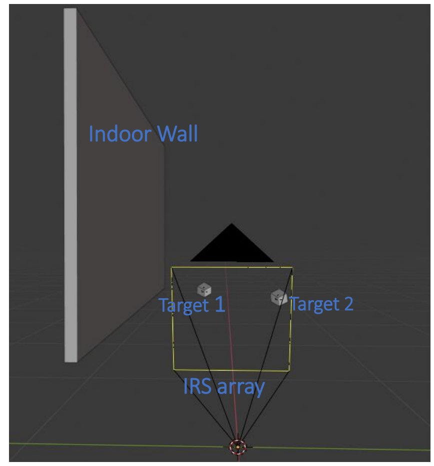


Fig. 7. The environment modeling of the simulated channel between the IRS array and the targets in Blender.

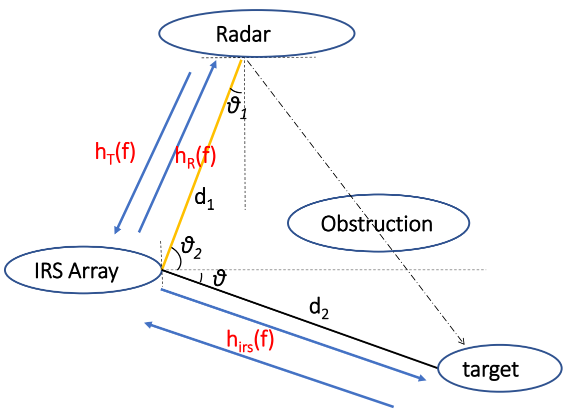


Fig. 6. The sub-channel representation of the IRS-radar link channel.

TABLE I
SENSOR CONFIGURATIONS

| Configurations | Values |
|---|---|
| Central frequency [GHz] | 77 |
| Number of Tx IRS units | 2/4 |
| Interval between neighboring Tx IRS units | $4\lambda$ |
| Number of Rx IRS units | 4 |
| Interval between neighboring Rx IRS units | $\lambda/2$ |
| Location of the radar | $[-3, 1, 1]$ |
| Central location of the IRS array | $[0, 0, 0]$ |
| Location of the target 1 | $[-1.1, 2.5, 0.5]$ |
| Location of the target 2 | $[0.4, 2, 0.45]$ |
| Bandwidth [GHz] | 1.8 |
| FMCW slope [MHz/us] | 30 |
| Frame/CPI duration [ms] | 40 |
| Number of blocks in one frame/CPI | 128 |
| Number of chirps in one block | MN |
| Sampling rates [MHz] | 10 |
| Number of IF samples for one chirp | 256 |

where $\boldsymbol{h}_{R,n}$ and $\boldsymbol{h}_{T,m}$ are the channel of the $n$th IRS unit to the radar and the radar to the $m$th IRS unit, respectively. The locations of the radar and IRS are static and known, hence $\boldsymbol{h}_{T,m}(\hat{l}, n_s)$ and $\boldsymbol{h}_{R,n}(\hat{l}, n_s)$ can be calculated (without the Doppler term) as

$$\boldsymbol{h}_{T,m}(\hat{l}, n_s) = A_{T,m} \exp\{j2\pi(\frac{2\mu d_1}{c}\frac{n_s - 1}{F_s})\}, \tag{19}$$

$$\boldsymbol{h}_{R,n}(\hat{l}, n_s) = A_{R,n} \exp\{j2\pi(\frac{2\mu d_1}{c}\frac{n_s - 1}{F_s})\}, \tag{20}$$

where amplitude calculation is the angle and frequency dependent, while already papers elaborate the signal strength enhancement via IRS in [7]. The two-way channel between the target and the IRS array can be entirely calculated in the Blender-based simulator as shown in Fig.7 using the formula below

$$\boldsymbol{h}_{irs,m,n}(\hat{l}, n_s) = A_{irs,m,n} \exp\{j2\pi( \frac{2\mu(R_{m,n} - d_1)}{c}\frac{n_s - 1}{F_s} - f_D(\hat{l} - 1)T_b + \phi_1)\}, \tag{21}$$

where the amplitude $A_{irs,m,n}$ and the range $R_{m,n}$, can be obtained directly by the rendering of the environmental model in Blender, and the Doppler velocity is calculated by the ratio of distance difference of two frames and the time interval of two frames.

The other important sensor configuration parameters are shown in Table I. It is worth mentioning that, the simulation of this work lies in the validation of range and angle estimation, hence the normalized amplitudes are used in estimation. By applying the fast Fourier transform (FFT) to each dimension of the channel, the range-angle maps are shown by Fig.8 and Fig.9, which show the simulated results of radar estimation assisted by $2$ Tx $4$ Rx IRS units and $4$ Tx $4$ Rx IRS units, respectively. We have to notice that, the range here refers to the distance from the target via the IRS array to the radar, and the angle is the AOA at the IRS array side.

From both the two range-angle maps, we could observe the target $1$ is at a distance of around $6$ meters with an angle around $-15$ degree, while the target $2$ is at a distance of around $5.5$ meters with an angle around $20$ degree, which are exactly

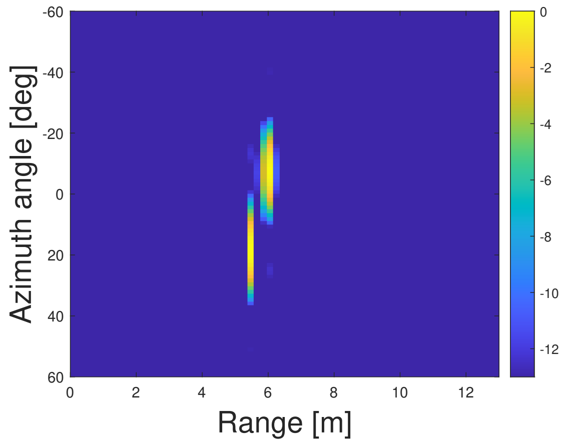


Fig. 8. The angle estimation of targets by a 2 by 4 IRS array.

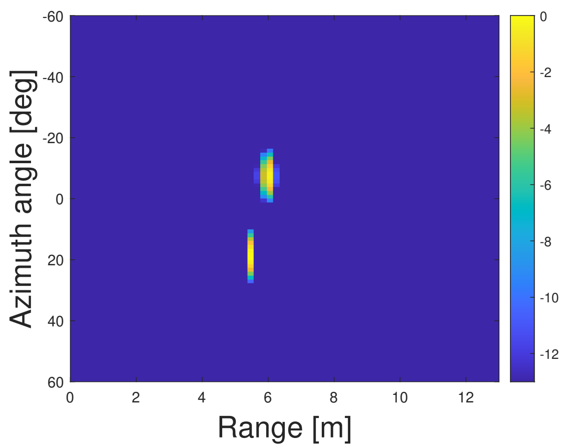


Fig. 9. The angle estimation of targets by a 4 by 4 IRS array.

matching with the scenario settings in Fig.5 and Table. I, validating the correctness of the proposed framework. Besides, by doubling the number of virtual arrays in the IRS units, the angle resolution improves approximately two times in Fig.9 than the angle resolution in Fig.8. However, one CPI block consists of $M$ by $N$ chirps, where $M$ and $N$ are the numbers of TX and Rx IRS units, respectively, hence increasing the number of arrays could improve the angle resolution, while costing more power.

## IV. Conclusions

In the NLoS scenarios, the MIMO operation of a radar is not necessary for angle estimation; instead, an IRS array can provide a delay difference due to the AoA of the target. This paper proposed a TCS-modulated IRS-aided radar localization framework, where the IRS array can be divided into a number of Tx IRS units and Rx IRS units. With each Tx and Rx IRS unit working in TDM mode, the signals containing angle information can be separated at the radar side using non-overlapping time slots. Simulation results show the merits of the range-angle estimation of the proposed methods. Furthermore, by increasing the number of IRS units, the approach obtains higher angle resolution. However, it will cost more time slot/power. Hence we need to design the proper number of IRS units according to application requirements.

## Acknowledgment

This work was supported by the Luxembourg National Research Fund (FNR) through the BRIDGES project MASTERS under grant BRIDGES2020/IS/15407066.

## References

[1] T. Wei, L. Wu, K. V. Mishra, and M. R. B. Shankar, “Multiple IRS-assisted wideband dual-function radar-communication,” in *2022 2nd IEEE International Symposium on Joint Communications & Sensing (JC&S)*, 2022, pp. 1–5.

[2] Y. Han, S. Zhang, L. Duan, and R. Zhang, “Double-IRS aided MIMO communication under LoS channels: Capacity maximization and scaling,” *IEEE Transactions on Communications*, vol. 70, no. 4, pp. 2820–2837, 2022.

[3] K. Keykhosravi, B. Denis, G. C. Alexandropoulos, Z. S. He, A. Albanese, V. Sciancalepore, and H. Wymeersch, “Leveraging RIS-enabled smart signal propagation for solving infeasible localization problems,” 2022.

[4] X. Wang, M. S. Mirmoosa, V. Asadchy, and S. Tretyakov, “Electromagnetic phenomena in time-modulated metasurfaces,” in *2022 Sixteenth International Congress on Artificial Materials for Novel Wave Phenomena (Metamaterials)*, 2022, pp. 460–462.

[5] A. C. Tasolamprou, A. Pitilakis, S. Abadal, O. Tsilipakos, X. Timoneda, H. Taghvaee, M. Sajjad Mirmoosa, F. Liu, C. Liaskos, A. Tsioliaridou, S. Ioannidis, N. V. Kantartzis, D. Manessis, J. Georgiou, A. Cabellos-Aparicio, E. Alarc$^3$n, A. Pitsillides, I. F. Akyildiz, S. A. Tretyakov, E. N. Economou, M. Kafesaki, and C. M. Soukoulis, “Exploration of intercell wireless millimeter-wave communication in the landscape of intelligent metasurfaces,” *IEEE Access*, vol. 7, pp. 122 931–122 948, 2019.

[6] X. Ma, M. S. Mirmoosa, and S. A. Tretyakov, “Complementary metasurfaces for guiding electromagnetic wave,” *IEEE Transactions on Antennas and Propagation*, vol. 69, no. 3, pp. 1815–1820, 2021.

[7] A. Aubry, A. De Maio, and M. Rosamilia, “RIS-Aided radar sensing in N-LOS environment,” in *2021 IEEE 8th International Workshop on Metrology for AeroSpace (MetroAeroSpace)*, 2021, pp. 277–282.

[8] Z. Esmaeilbeig, K. V. Mishra, and M. Soltanalian, “IRS-Aided radar: Enhanced target parameter estimation via intelligent reflecting surfaces,” in *2022 IEEE 12th Sensor Array and Multichannel Signal Processing Workshop (SAM)*, 2022, pp. 286–290.

[9] S. Ghotbi, M. Ahmadi, and K. Mohamedpour, “Moving target detection under spatially non-homogeneous clutter for airborne phased-MIMO radar,” in *2015 IEEE Radar Conference*, 2015, pp. 82–86.

[10] Y. Liu, L. Wu, M. Alaee-Kerahroodi, and B. S. M. R, “A 3D indoor localization approach based on spherical wave-front and channel spatial geometry,” in *2022 IEEE 12th Sensor Array and Multichannel Signal Processing Workshop (SAM)*, 2022, pp. 101–105.

[11] L. Zhang, X. Q. Chen, S. Liu, Q. Zhang, J. Zhao, J. Y. Dai, G. D. Bai, X. Wan, Q. Cheng, G. Castaldi *et al.*, “Space-time-coding digital metasurfaces,” *Nature communications*, vol. 9, no. 1, pp. 1–11, 2018.

[12] G. Wu, J. Dai, Q. Cheng, T. Cui, and C. Chan, “Sideband-free space-time-coding metasurface antennas,” *Nature electronics*, 2022.

[13] J. Lin Jr, Y.-P. Li, W.-C. Hsu, and T.-S. Lee, “Design of an FMCW radar baseband signal processing system for automotive application,” *SpringerPlus*, vol. 5, no. 1, pp. 1–16, 2016.

[14] V. Winkler, “Range doppler detection for automotive FMCW radars,” in *2007 European Radar Conference*, 2007, pp. 166–169.

[15] M. Ouza, M. Ulrich, and B. Yang, “A simple radar simulation tool for 3D objects based on blender,” in *2017 18th International Radar Symposium (IRS)*, 2017, pp. 1–10.

[16] R. F. da Costa, D. d. S. de Medeiros, R. Andrade, O. Saotome, and R. Machado, “General purpose radar simulator based on Blender cycles path tracer.”